

## QUANTIFYING SHORT AND LONG-TERM WEATHER PATTERN IMPACTS ON ARIDITY TRENDS IN EASTERN TEXAS USING AUTO REGRESSIVE TIME SERIES MODELING AND RANDOMIZATION

ROBERT KENNEDY SMITH<sup>1,\*</sup> AND DER-CHEN CHANG<sup>2,3</sup>

<sup>1</sup>*Department of Computer Science, Georgetown University, Washington DC, 20057, USA*

<sup>2</sup>*Department of Mathematics and Statistics, Georgetown University, Washington DC, 20057, USA*

<sup>3</sup>*Graduate Institute of Business Administration, College of Management, Fu Jen Catholic University, New Taipei City 242, Taiwan, ROC*

**ABSTRACT.** Climate model projections agree that warming air temperatures will exceed increases in the dewpoint temperature, causing lower relative humidities and increased soil moisture deficits across the U.S. South. Increased reference evapotranspiration ( $ET_0$ ) is projected to be greater than the enhanced rainfall associated with anthropogenic climate change in almost all areas of the contiguous U.S., leading to expanding aridity. Meanwhile, there is also model agreement that precipitation will fall at heavier rates under warmer conditions, leading to additional runoff, and thus less water absorption, even under drier overall conditions. Although it could be tempting to assume that projected changes in soil moisture will be a result of future average conditions (the average monthly amount of water absorbed by the soil minus the average monthly amount that evaporates), this does not account for evolving weather patterns, multiday extreme events, and other anthropogenic influences such as urban heat islands. This brief analysis quantifies how climate change has impacted these factors in the recent past in the U.S. State of Texas, providing a preliminary measurement of the weather pattern-related impacts of human-induced climate change.

**Keywords.** Climate change reference evapotranspiration, AR modeling process.

© Journal of Decision Making and Healthcare

### 1. INTRODUCTION AND BACKGROUND

According to results from Phases 5 and 6 of the Coupled Model Intercomparison Project (CMIP5 and CMIP6) used in the Fifth National Climate Assessment (Jay et al. 2023), rising temperatures will cause augmented reference evapotranspiration ( $ET_0$ ) rates to outweigh increases in precipitation in nearly all the contiguous U.S., with some exceptions in the Midwest (Payton et al. 2023). In Texas, projected midcentury annual precipitation totals are expected to decline, exacerbating increased  $ET_0$ -induced aridity. Models also forecast growth in extreme precipitation in the second half of the century (Lopez-Cantu et al. 2020), as explained by the Clausius-Clapeyron (CC) relationship. The combination of fewer days during which rain falls, more runoff from extreme events during which moisture cannot be fully absorbed – even by unsaturated soils, and growing vapor pressure deficits, makes model projections of more severe long-term and flash agricultural droughts highly confident (Brown et al. 2020; Gamelin et al. 2022; Steiner et al. 2018).

Coinciding with these trends, long and short-term weather patterns will also be affected by warming temperatures, although their effects on Texas drought are highly uncertain and variable. As one example, climatically-induced changes in the amplitude and seasonality of the El Niño-Southern Oscillation (ENSO) may make the region wetter during the winter months while stymieing the development of

\*Corresponding author.

E-mail address: rks21383@gmail.com (Robert Kennedy Smith), chang@georgetown.edu (Der-Chen Chang)

Accepted: October 21, 2024.

summertime tropical cyclone formation in select years, resulting in more pronounced periods of wetness and dryness (Alizadeh 2022) and additional stress on water systems. Another example is provided: climate change will also affect tropical system seasonality, intensity, translation speed, and track (Feng, X 2021; Yamaguchi et al, 2020; Wu et al., 2022). While the net result may be more flooding attributable to tropical cyclones in the vicinity of the Texas coastline, it does not necessarily translate to overall wetness during the growing season (Hassanzadeh 2020), so even models with high degrees of seasonal precision may not capture offsetting pattern changes. Texas also lies near the transition area between the subtropics and midlatitudes, where observed and modeled changes in tropical cyclone speed are less clear than for other areas (such as the mid-Atlantic where there is a high degree of confidence that the northward displacement of the midlatitude jet has resulted in slower moving, wetter storms) (Zhang 2020).

Although the individual reporting stations analyzed in this study do not show universal, statistically significant ( $p$  value  $< 0.10$ ) increases in precipitation between 1973 and 2023, interpolated climate divisional data (Vose et al. 2014) show long-term positive historical precipitation trends in most of the State. All stations are located East of the 100th parallel, where more than 75 percent of the land area has experienced between a 10 and 20 percent increase in precipitation over the past century (Nielsen-Gammon et al. 2020). Model projections showing a reverse in these trends by the middle of the 21st century with accelerated soil dryness will also influence weather patterns. While they show an increased probability of heat dome-like circulation with warmer temperatures, dry soil moisture further enhances high-pressure anomalies, strengthening the descending motion that suppresses rainfall and cloud cover, thus reinforcing the pattern (Zhang et al. 2023). Such feedback mechanisms become essential for drought mitigation planning as previously low-probability events become more regular occurrences.

Earlier studies examining precipitation patterns (Breinl et al. 2020; Smith and Chang 2020) in the United States from 1958 to 2018 showed the duration of dry and wet spells increasing in Texas, with dry periods lengthening at a faster, more uniform rate across the state. While the paper only used rainfall frequency and did not address agricultural drought, the concurrent rise in reference evapotranspiration rates would exacerbate aridity stress on agriculture, without necessarily reducing flooding-related damage. In this analysis, temporal changes in water permeating into and evaporating from the ground are combined, showing the agricultural impact of weather pattern changes.

## 2. METHODOLOGY

This study uses existing models and methods to quantify the impact of short and long duration patterns on drought in the Central and Eastern parts of Texas. The daily averages of four climate parameters, wind speed ( $m/second$ ), solar radiation [ $MJm^{-2}/day$ ], air temperature ( $^{\circ}C$ ), and dewpoint temperature ( $^{\circ}C$ ), were obtained for 16 stations (Figure 1) using data from the National Centers for Environmental Information (NCEI)<sup>1</sup> and the North American Regional Reanalysis (NARR), an extension of the NCEP Global Reanalysis<sup>2</sup>, along with aggregated daily precipitation from official hourly observations. The data are quality controlled and have few missing records.

In isolated instances where a record was missing, nearby stations within the NCEI network provided a substitute value. Along with latitude and elevation, these are imputed into the FAO-56 Penman-Monteith Equation (Zontarelli et al. 2010) to calculate how much moisture leaves a well-watered reference fescue grass surface each day between 1 January 1973 and 30 June 2023, with reference evapotranspiration ( $ET_0$ ) given by the following:

1. <https://data.noaa.gov/dataset/dataset/global-surface-summary-of-the-day-gsod>;  
<https://www.ncdc.noaa.gov/data-access/land-based-station-data/land-based-datasets/global-historical-climatology-network-ghcn>

2. <http://climateengine.org/>

$$ET_0 = \frac{0.408(R_0 - G) + \gamma \frac{900}{T+237} u_2(e_s - e_a)}{\Delta + \gamma(1 + 0.34u_2)} \quad (2.1)$$

where  $\Delta$  is the slope of the saturation vapor pressure curve,  $R_0$  is the net radiation at the crop surface,  $G$  is the soil heat flux density,  $\gamma$  is the psychrometric constant,  $T$  is the mean daily air temperature,  $u_2$  is the wind speed,  $e_s$  is the saturation vapor pressure, and  $e_a$  is the actual vapor pressure.

Station Identifier	Station Name	Latitude	Longitude
1	Abilene Regional Airport, TX	32.41° N	99.68° W
2	Wichita Falls Municipal Airport, TX	33.98° N	98.49° W
3	San Antonio International Airport, TX	29.54° N	98.48° W
4	McAllen International Airport, TX	26.18° N	98.25° W
5	Mathis 4 SSW, TX	28.04° N	97.87° W
6	Brownsville SPI Int'l Airport, TX	25.91° N	97.42° W
7	Waco Regional Airport, TX	31.62° N	97.23° W
8	Dallas/Ft. Worth Int'l Airport, TX	32.90° N	97.02° W
9	Victoria Regional Airport, TX	28.84° N	96.92° W
10	Palacios Municipal Airport, TX	28.72° N	96.25° W
11	Bush Intercontinental Airport, TX	29.98° N	95.36° W
12	William Hobby Airport, TX	29.64° N	95.28° W
13	Angelina County Airport, TX	31.24° N	94.75° W
14	Brooks Regional Airport, TX	29.95° N	94.02° W
15	Texarkana Regional-Webb Field, TX	33.46° N	93.99° W
16	Shreveport Regional Airport, LA	32.45° N	93.82° W

FIGURE 1. Station Location

Using the USDA National Resources Conservation Service's online soil survey, a weighted average of the moisture holding capacity in the top meter of soil at each of the 16 observation stations was obtained. The ability of the grassy vegetation to draw water at the reference rate continues until the readily available water supply is exhausted. Root systems will then draw from the total available water supply at a slower rate, continuing to lessen as the grass becomes increasingly parched (Wright 1993). Days during which precipitation falls replenish soil moisture, until the overall field capacity is exceeded. The surplus is assumed to be lost under these saturated conditions, although it can percolate through the ground and recharge aquifers or be held in collection areas for future utilization (Kirshna et al. 1987).

The algorithm deployed for this analysis measuring potential irrigation demand discharges 12.7 mm of water (0.5") whenever the readily available supply is depleted. On rainy days when less than that quantity falls, the difference is assumed to be discharged while no irrigation activity occurs during days when more than 12.7 mm was observed. The criterion is repeated on each subsequent day, with the monthly aggregate supplemental water demand calculated.

Observed trends in irrigation water demand and  $ET_0$  over the period from 1 January 1973 to 30 June 2023 were calculated with autoregressive (AR) time series modeling on seasonally-adjusted monthly

totals in  $R$ . After the initial model of order zero, a correlogram for lags 1 – 20 was created and visually inspected. Whenever the first lag exceeded the significance bounds of  $|0.2|$ , the model’s order was increased by one and the cycle was repeated until no autocorrelation was observed. This is expressed as

$$z_t = \alpha_1 z_{t-1} + \alpha_2 z_{t-2} + \dots + \alpha_p z_{t-k} + w_t \tag{2.2}$$

where  $w_t$  is white noise;  $k$  ranged from 0 to 4 throughout the analysis. While watering demand trends were, on average, of greater magnitude than those of  $ET_0$ , only eight observation stations had statistically significant trends ( $p$  value  $< 0.1$ ). Therefore, four additional stations with  $p$ -values greater than 0.1 but less than 0.3 were also included in the stage 2 (weather pattern) analysis. All 12 stations had positive  $ET_0$  and irrigation water demand trends.

To determine if changes in short-term weather patterns are exacerbating drought, as measured through irrigative water demand, daily precipitation observations within each month were randomized and the algorithm recalculated aggregated monthly supplemental water demand. The  $AR$  modeling process was again conducted. This was repeated for nine additional randomizations. The average of the trend magnitude was compared to the original, observed value. Additionally, the impact of long-term weather patterns was measured by randomizing the daily precipitation records in three-year blocks. For example, block 1 contained randomized daily rainfall records from January 1973-1975, and block 2 contained data from the first three consecutive Februaries. Since the number of like months in the analysis period was not divisible by 3, the final blocks contained randomizations from two or four years (as there were 53 instances of January-June and 52 instances of July-December). As earlier, nine subsequent randomizations were performed, with the trends averaged and compared to the original observations.

### 3. RESULTS AND DISCUSSION

Warming has increased reference evapotranspiration rates at all 16 observation locations, with 12 locations showing statistically significant trends in  $ET_0$  over the analysis period [mean: 1.6  $mm/decade$ , range: 0.7 – 3.1  $mm/decade$ ]. Precipitation trends at these locations were mixed, with only one of the 12 exhibiting statistical significance. For irrigative water demand, all 12 locations had positive trends, seven of which were statistically significant. The demand trend mean for this sample was 2.2 $mm^{-1}$  decade [range: 0.7 – 3.6  $mm/decade$ ]. A different set of stations comprised those with watering trend  $p$ -values below 0.3. This subgroup had a higher mean demand trend [2.4  $mm/decade$ , range: 1.4 – 3.6  $mm/decade$ ] and the criterion excluded three of the four stations east of the Houston metropolitan area. The mean, seasonally-adjusted monthly demand was 71.6  $mm$  and ranged from 33.7  $mm$  per month at William Hobby Airport to 116.3  $mm$  per month at McAllen International Airport.

Monthly watering demand from the set of 10 monthly randomization simulations was expectedly lower across all stations (mean: 69.2  $mm$ ), as multiday consecutive events during which water runs off saturated soils are spaced out within each month. If evolving short-term weather patterns were not affecting aridity, watering demand trend magnitudes would be the same with the randomized data as what was observed with historical values. Instead, all 12 stations exhibited smaller trends, with an overall mean of 2.0  $mm/decade$  [range: 1 – 3.2  $mm/decade$ ]. When precipitation data is further randomized in three-year monthly blocks, all 12 locations have lower water demand trends [mean: 1.7  $mm/decade$ , range: 0.7 – 3.1  $mm/decade$ ] relative to trends from the historical data and intramonth randomizations. Figure 2 shows the 12-station subsample (moving East from the left). The contribution of short and long-term weather patterns to soil moisture deficits over the analysis period is the height of the gray and orange portions of each station’s bar, respectively.

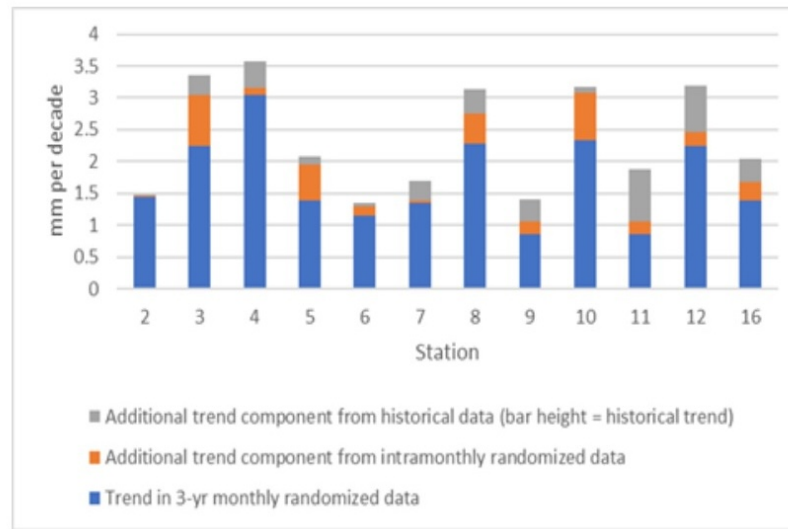


FIGURE 2. Trend in Irrigative Water Demand (January 1974 - June 2023)

Both sets of 10 randomizations were regressed in  $R$  individually for each station, as the autoregressive order was iteratively determined by examining the models' residuals. Since this was not a preprogrammed algorithm designed to run several dozen iterations, each station's average may be slightly skewed from the horizontal asymptote representing the true mean value if the number of iterations were to have gone indefinitely. Figure 3 shows, as a percentage of the historical watering demand trend, average values for each station as an additional randomization is added to the set. The two stations with the highest volatility between runs (5 and 8) did not exhibit statistically significant trends. Nonetheless, when the trends from the 10 randomizations are averaged, they are well below those derived from historical data for all 12 stations. The mean trend magnitude for the randomized 12 station subsample is 71 percent of the observed trend [range: 43% – 93%], which means that 29 percent of the historical increased water demand has originated from changes in short and long-term precipitation patterns rather than differences in the overall amount of precipitation that has fallen, evolving seasonal rainfall patterns, and the increased rate of reference evapotranspiration.

While climate model forecasts are adept at accounting for expected increases in precipitation intensity and flooding risk from additional runoff (McPherson et al. 2023), as well as exacerbated drought from the evolving conditions previously listed (Zhang et al. 2021), the understanding of how weather pattern changes affect soil moisture levels is more complicated and uncertain (Hawkins et al. 2020) since longer periods of entrenched patterns can simultaneously cause wetter seasonal conditions with deeper droughts. Higher degrees of precision in understanding how warmer conditions affect overall circulation can better estimate risk and motivate proper infrastructure investment. This analysis only accounts for runoff attributable to daily events, and therefore overestimates the amount of water absorbed into the ground when assuming unlimited permeability until saturation is reached. Documented increases in hourly rainfall rates, found to be highly correlated with temperature (Ali et al. 2021), would undoubtedly further exacerbate simultaneous flood and drought risk. A recent anecdote is provided to illustrate the point: 2017 was the wettest year on record in Houston, TX (2,024mm/79.69" fell), during which Hurricane Harvey devastated the city (Trenberth et al. 2018), yet the U.S. Drought Monitor classified Harris County as abnormally dry during late May and late November of that year. Especially as flash droughts proliferate (Yuan 2023), vegetation may be vulnerable to damage from flooding and arid conditions within the same month.

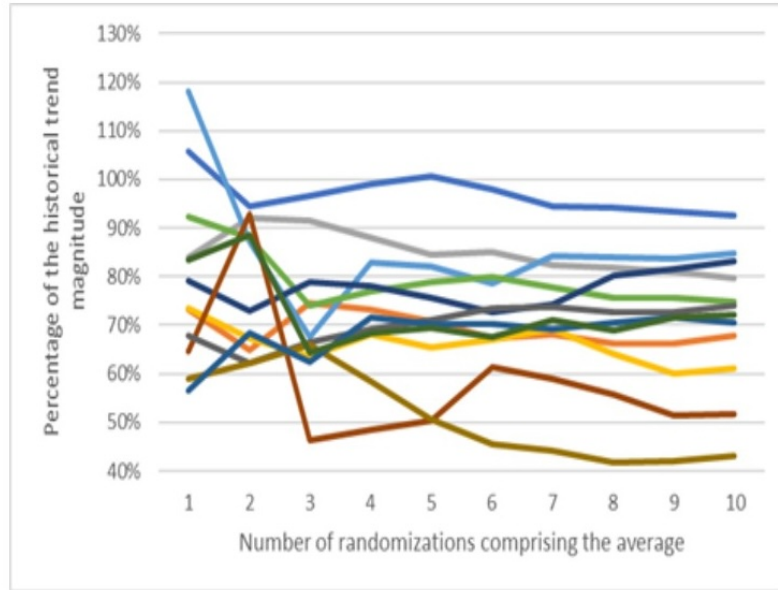


FIGURE 3. Three-year monthly block average randomization values by station, as a percentage of the historical trend

In addition to weather pattern changes, reference evapotranspiration, precipitation amount and seasonality, microclimatic factors can impact soil moisture levels. A recent global-scale assessment comparing urban areas to their outlying surroundings, showed, by a 2 : 1 margin, U.S. cities are wetter than nearby undeveloped areas (Sui 2024). Odds increase when only cities without heavy topographical variance are considered, such as the selected locations in Texas. In the Sui analysis, Houston was eighth out of the world’s 100 largest metro areas for enhanced precipitation, receiving more than 10 percent (approximately 130mm) of the rainfall observed in the immediate vicinity. Urban heat islands have been known to enhance convective events, especially at coastal locations that experience an afternoon sea breeze during the warm season (Shepherd et al. 2011), however other factors can wet and dry cities such as tall buildings and impermeable surface cover. As the eastern half of Texas has developed over the analysis period, it is possible some of the pattern entrenchment is due to the local factors that lie outside of global circulation modeling.

#### 4. CONCLUSION

While the increased aridity in Eastern Texas is largely explained by higher rates of reference evapotranspiration from warming and evolving precipitation amounts, isolating the impact from short and long-term weather patterns show their impact in accelerating soil moisture scarcity. This paper does not seek to identify the causes of the deepening pattern entrenchment, but rather provides a measure of its manifestation. While comprehensive climate reports cover aridification, the discussion is usually limited to evapotranspiration, evolving seasonal precipitation patterns, and moisture from named tropical cyclones. The other factors, of which there may be several, including those partially offsetting each other, will be relevant to ensure accurate climate forecasts that will inform policy decisions.

## STATEMENTS AND DECLARATIONS

The authors declare that they have no conflict of interest, and the manuscript has no associated data.

## ACKNOWLEDGMENTS

Der-Chen Chang's research is partially supported by a National Science Foundation grant (DMS-1408839) and the McDevitt Endowment Fund at Georgetown University.

## REFERENCES

- [1] H. Ali, H. Fowler, G. Lenderink, E. Lewis, and D. Pritchard. Consistent large-scale response of hourly extreme precipitation to temperature variation over land. *Geophysical Research Letters*, 48:e2020GL090317, 2021.
- [2] O. Alizadeh. Amplitude, duration, variability, and seasonal frequency analysis of the El Niño-southern oscillation. *Climatic Change*, 174:20, 2022.
- [3] V. Brown, B. Keim, , and A. Black. Trend analysis of multiple extreme hourly precipitation time series in the Southeastern United States. *Journal of Applied Meteorology and Climatology*, 59:427-442, 2020.
- [4] X. Feng, N. Klingaman, and K. Hodges. Poleward migration of western North pacific tropical cyclones related to changes in cyclone seasonality. *Nature Communications*, 12:6210, 2021.
- [5] B. Gamelin, J. Feinstein, J. Wang, J. Bessac, E. Yan, and V. Kotamarthi. Projected U.S. drought extremes through the twenty-first century with vapor pressure deficit. *Scientific Reports*, 12:8615, 2022.
- [6] P. Hassanzadeh, C. Lee, , E. Nabizadeh, S. Camargo, D. Ma, and Y. Laurance. Effects of climate change on the movement of future landfalling Texas tropical cyclones. *Nature Communications*, 11:3319, 2020.
- [7] E. Hawkins, D. Frame, L. Harrington, M. Joshi, A. King, M. Rojas, and R. Sutton. Observed Emergence of the climate change signal: From the familiar to the Unknown. *Geophysical Research Letters*, 47:e2019GL086259, 2020.
- [8] J. Krishna, G. Arkin, and R. Martin. Runoff impoundment for supplemental irrigation in Texas. *Journal of the American Water Resources Association*, 23:1057-1061, 1987.
- [9] T. Lopez-Cantu, A. Prein, and C. Samaras. uncertainties in future U.S. extreme precipitation from downscaled climate projections. *Geophysical Research Letters*, 47:e2019GL086797, 2020.
- [10] A. K. Jay, A. R. Crimmins, C. W. Avery, T. A. Dahl, R. S. Dodder, B. D. Hamlington, A. Lustig, K. Marvel, P. A. Méndez-Lazaro, M. S. Osler, A. Terando, E.S. Weeks, and A. Zycherman: Chapter 1. Overview: Understanding risks, impacts, and responses. In: Fifth National Climate Assessment (NVA5). A. R. Crimmins, C. W. Avery, D. R. Easterling, K. E. Kunkel, B. C. Stewart, and T. K. Maycock, editors, *U.S. Global Change Research Program*, pages 1-47, Washington, DC, USA, 2023.
- [11] R. A. McPherson, P. A. Fay, S. G. Alvarez, D. Bertrand, T. L. Broadbent, T. Bruno, A. Fares, B. McCullough, G. W. Moore, B. Moorhead, L. Patiño, A. Petersen, N. G. Smith, J. L. Steiner, A. Taylor, and T. Warziniack. Chapter 26. southern great Plains. In: Fifth National Climate Assessment (NCA5). A. R. Crimmins, C. W. Avery, D. R. Easterling, K. E. Kunkel, B. C. Stewart, and T. K. Maycock, Editors, *U. S. Global Change Research Program*, Washington, DC, USA, 2023.
- [12] J. W. Nielsen-Gammon, J. Banner, B. Cook, D. Tremaine, et al. Unprecedented drought challenges for Texas water resources in a changing climate: what do researchers and stakeholders need to Know?. *Earth's future*, 8:e2020EF001552, 2020.
- [13] E. A. Payton, A.O. Pinson, T. Asefa, L. E. Condon, L.-A. L. Dupigny-Giroux, B. L. Harding, J. Kiang, D. H. Lee, S. A. McAfee, J. M. Pflug, I. Rangwala, H. J. Tanana, and D. B. Wright, 2023: Chapter 4. Water In: Fifth National Climate Assessment (NCA5), A. R. Crimmins, C. W. Avery, D. R. Easterling, K. E. Kunkel, B. C. Stewart, and T. K. Maycock, Editors, *U.S. Global Change Research Program*, Washington, DC, USA, 2023.
- [14] J. Shepherd, M. Carter, D. Messen, and S. Burian. The impact of urbanization on current and future coastal precipitation: a case study for Houston. *Environment and Planning B: Planning and Design*, 37(2):284-304, 2010.
- [15] R. Smith and D. Chang. Utilizing recent climate data in eastern Texas to Calculate trends in measures of aridity and estimate changes in watering demand for landscape preservation. *Journal of Applied Meteorology and Climatology*, 59:143-152, 2020.
- [16] J. Steiner, D. Briske, D. Brown, and C. Rottler. Vulnerability of southern plains agriculture to climate change. *Climatic Change*, 146:201-218, 2018.
- [17] X. Sui, Z. Yang, M. Sheperd, and D. Niyogi. Global scale assessment of urban precipitation anomalies. *Proceedings of the National Academy of Sciences*, 38:e2311496121, 2024.
- [18] K. Trenberth, L. Cheng, P. Jacobs, Y. Zhang, and J. Fasullo. Hurricane Harvey links to ocean heat content and climate change adaptation. *Earth's Future*, 6:730-744, 2018.

- [19] R. Vose, S. Applequist, M. Squires, I. Durre, M. Menne, C. Williams, C. fenimore, K Gleason and D. Arndt. Improved historical temperature and precipitation time series for U.S. climate divisions. *Journal of Applied Meteorology and Climatology*, 53:1232-1251, 2014.
- [20] J. Wright. *Nongrowing season ET from irrigated fields. Management of Irrigation and Drainage Systems: Integrated Perspectives*, American Society of Civil Engineers, 1005–1014, 1993.
- [21] L. Wu, H. Zhao, C. Wang, J. Cao, and J. Liang. Understanding of the effect of climate change on tropical cyclone intensity: a review. *Advances in Atmospheric Sciences*, 39:205-221, 2022.
- [22] M. Yamaguchi, J. Chan, I. Moon, K. Yoshida, and R. Mizuta. Global warming changes tropical cyclone translation speed. *Nature Communications*, 11:47, 2020.
- [23] X. Yuan, Y. Wang, P. Ji, P. Wu, J. Sheffield, and J. Otkin. A global transition to flash droughts under climate change. *Science*, 380:187-191, 2023.
- [24] F. Zhang, J. Biederman, M Dannenberg, D. Yan, S. Reed, and W. Smith. Five decades of observed daily precipitation reveal longer and more variable drought events across much of the Western United States. *Geophysical Research Letters*, 48:e2020GL092293, 2021.
- [25] G. Zhang, H. Murakami, T. Knutson, R. Mizuta, and K. Yoshida. Tropical cyclone motion in a changing climate. *Science Advances*, 6:eaaz7610, 2020.
- [26] X. Zhang, T. Zhou, W. Zhang, L. Ren, J. Jiang, S. Hu, M. Zuo, L. Zhang, and W. Man. Increased impact of heat domes on 2021-like heat extremes in North America under global warming. *Nature Communications*, 14:1690, 2023.
- [27] L. Zontarelli, M. D. Dukes, C. C. Romero, K. W. Migliaccio, and K. T. Morgan. Step by step calculation of the Penman-Monteith evapotranspiration (FAO-56 method). *Institute of Food and Agricultural Sciences, University of Florida*, 8:AE459, 2010.